Radio Channel Properties for Vehicular Communication: Merging Lanes Versus Urban Intersections

Abbas, Taimoor; Bernado, Laura; Thiel, Andreas; F. Mecklenbräuker, Christoph; Tufvesson, Fredrik

Published in:
IEEE Vehicular Technology Magazine

DOI:
10.1109/MVT.2013.2281676

2013

Radio Channel Properties for Vehicular Communication: Merging Lanes vs. Urban Intersections

Taimoor Abbas, *Student Member, IEEE,* Laura Bernadó, *Member, IEEE,* Andreas Thiel,
Christoph Mecklenbräuker, *Senior Member, IEEE,* and Fredrik Tufvesson, *Senior Member, IEEE*

VEHICLE-TO-VEHICLE (V2V) communication is a challenging but fast growing technology. It has a potential to enhance the road safety by supporting the driver to avoid collisions in the basic maneuvers such as crossing street intersections, changing lanes, merging on a highway, and driving safely in blind turns. The significance of V2V safety applications increases further where the visual line-of-sight (LOS) is unavailable due to buildings, roadside sound berms or small hills at an intersection point of two or more roads intersecting at a certain angle, e.g. merging lanes, the entrance or exit ramps on a highway, or four-way street intersections. The reliability of V2V safety applications, which use IEEE 802.11p as the underlying communication technology [1], highly depend on the quality of the communication link, which rely upon the properties of the propagation channel. Therefore, understanding the properties of the propagation channel becomes extremely important.

A number of research outcomes have been published covering many aspects of V2V propagation channels [2]. In this paper results for V2V channel characterization based on measurements conducted for merging lanes on a highway, and four-way street interception scenarios are presented. The importance of different propagation mechanisms in non-line-of-sight (NLOS) situations and the impact of antenna radiation pattern on the total received power in LOS situations is highlighted for these scenarios. These metrics are of particular interest for V2V safety critical applications such as collision avoidance application.

Some theoretical, simulation and measurement based studies have been conducted in the past dealing with the merging lane scenarios [3]–[7], in which the merging/changing lane control algorithms, systems and channel properties are discussed, and simulation results are provided to show how to avoid possible collisions. Similarly, channel characterization and path-loss models for the situation when two cars are approaching an intersection with a risk of collision have been presented in [8], [9].

Vehicles that are approaching a street intersection or merging on a highway often have NLOS from the vehicles in the other street or road because the visual LOS is blocked by nearby buildings or objects. In such situations scattering of radio waves, i.e., reflection, diffraction, and refraction, implicitly enable NLOS reception. Moreover, merging lanes occur often in highway or rural environments, this is why there are few big objects in the surrounding that can contribute to increase the scattering. Similarly, some street intersections, often called open intersections which have one big building that block the LOS and only few scattering objects in the surrounding. Thus, NLOS reception in merging lane and open intersection scenarios could probably be very bad.

In contrary to NLOS, LOS reception can go really bad if the antenna pattern has a dip in the direction-of-departure (DOD) or direction-of-arrival (DOA) of the LOS path. In open environments the probability of losing the packets due to bad reception is even higher because there are no other significant scatterers to carry the signal power. Thus an antenna pattern should be designed such that it has good coverage in all directions or multiple antennas should be considered. Multiple antennas mounted at different locations on the car can help to exploit diversity and combat shadow fading [10].

In many simulation studies the antennas are assumed to be isotropic, radiating equal power in all directions, and the communication range is assumed to be a circle around the TX, which is a perfect condition for reception but its not the case in reality. The communication range depends on a number of factors involving the antenna radiation pattern, location of the antenna on the car, the traffic density, obstacles such as buildings and vehicles, and the transmitted power. The antenna pattern is one of the major limiting factors and to perform a realistic simulation studies it is necessary to use somewhat realistic antenna patterns.

To emphasize this, measurements data is collected and analyzed for both scenarios, and results for this antenna-channel interaction are presented. To identify the important propagation mechanisms, a directional analysis is performed using a high resolution space-alternating expectation maximization algorithm (SAGE) [11] for selected time-snapshots. Particular focus is put on the LOS component as it carries most of the received power. The DOA/DOD estimates are presented to show how the antenna pattern can affect the received signal strength, when the LOS component is received at an angle where the antenna has a lower gain.

I. V2V Measurement Setup

V2V channel measurements were conducted using the RUSK Lund channel sounder that performs multiple-input multiple-output (MIMO) measurements based on the switched-array principle [12]. For the measurements, two standard hatch-back style cars were used and the four-element

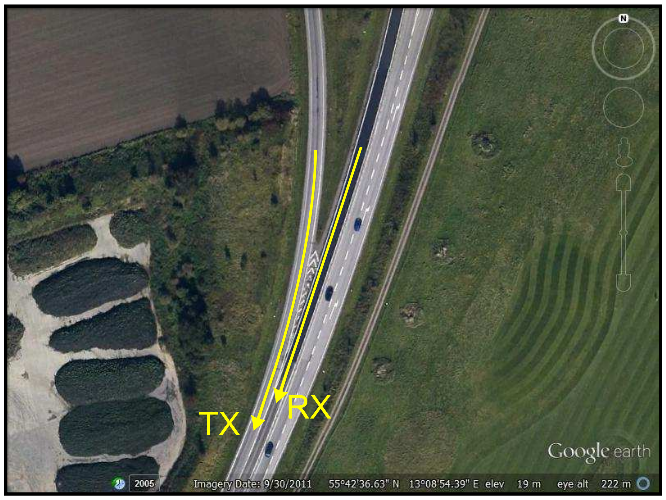

Fig. 1. Google Earth™ [14] aerial image shows the investigated merging lane scenario outside the city of Lund. The TX enters the highway while RX is approaching the merging point on the highway. (N $55°42'36''$, E $13°8'53''$)

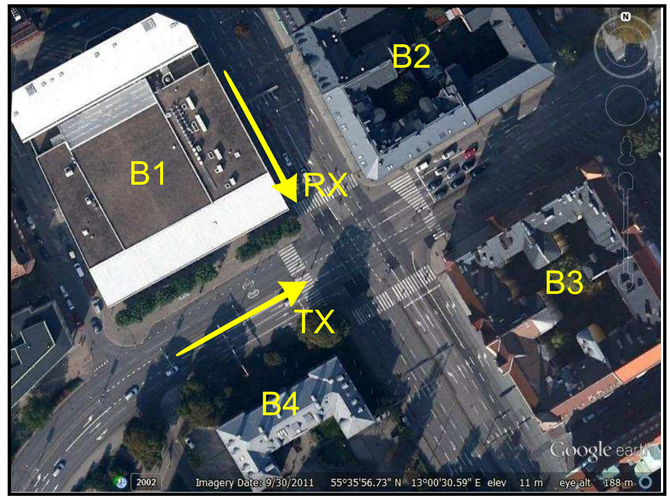

Fig. 2. Google Earth™ [14] aerial image shows the investigated four-way intersection scenario in Malmö where both the TX and RX are approaching the intersection. Four buildings at each corner B1, B2, B3 and B4 are marked clockwise starting from the top left corner, respectively. (N $55°35'56''$, E $13°0'30''$)

antenna arrays were mounted on the roof. The height of each antenna array was $1.73\,\mathrm{m}$ from the ground. The channel sounder sampled the 4×4 MIMO time-varying channel transfer function $H(f,t)$ over a $240\,\mathrm{MHz}$ of measurement bandwidth centered at $5.6\,\mathrm{GHz}$. The temporal sampling and the measurement duration were set to $307.2\,\mu$s and $20\,$s, respectively, with a test signal length of $3.2\,\mu$s. The 4×4 MIMO antenna arrays were used to exploit diversity as the different TX-RX pairs give rise to different directional links. These arrays were designed specifically for V2V communication [13]. Each element of the arrays has a directional antenna gain such that the antenna pattern of element $1, 2, 3$ and 4 have their main gain pointing to the left-side, backward, forward and to the right-side of the car, respectively. In the subsequent analysis we consider all four elements of the TX array such that the transmitter has somewhat omni-directional gain and then the power received at the element-1 is compared against the element-2 of the RX array.

To keep track of the positions of the transmitter (TX) and receiver (RX) cars, during the measurements, each vehicle logged the GPS coordinates and videos were recorded through the windshield. This data was combined with the measurement data, in order to identify the important scatterers in the post-processing.

A. Scenario Description

Merging lanes: The merging lane scenario at a highway is characterized by the roads that are used to merge two traffic flows into one, e.g., entrance or exit ramps. An important aspect of this scenario is the possibility of an obstructed LOS path due to the slope and the orientation of the terrain, or the presence of sound barriers, buildings or trees between the intersecting roads. This scenario is similar to the urban street crossings scenario [8], but with slightly more difficult channel conditions in the absence of the LOS due to open surroundings, availability of fewer scatterers and higher vehicle speeds. In order to draw conclusions on the importance of scatterers in the absence of LOS, two types of measurements were conducted for the merging lanes scenario: 1) Vehicles merging at an entrance ramp, when the RX car was driving on the highway and the TX car was entering on the highway; 2) Vehicles splitting at an exit ramp, where the RX car was exiting from the highway and the TX car continued driving on the highway. In this paper we focus mainly on entrance ramps (see Fig. 1), since this is the most important case in terms of collision avoidance and the experiences learned from these results can be applied on exit ramps.

Several measurements were made and during each measurement the RX car was moving on the highway and the TX car was entering on the highway from the entrance ramp. Both the cars were moving at the speed of $20-28\,\mathrm{m/s}$ ($70-100\,\mathrm{km/h}$). Two measurements are chosen for the analysis;

Scenario-1**:** when the TX enters the highway and remains behind the RX, which is already driving on the highway, and there are other vehicles driving by.

Scenario-2**:** when the TX enters the highway and remains in front of the RX, which is already driving on the highway, and there are no vehicles around.

Four-way Intersection: In order to highlight the importance of scattering objects in NLOS situations the measurement results for a four-way intersection have also been included. A four-way intersection scenario is characterized by that four urban-streets of varying widths meet at a certain point, such that the visual LOS between cars on the intersecting streets is blocked by building of certain height situated at the corner of the intersection. There are buildings, trees, light poles, and street signs at random location. These objects are expected to provide many additional multi-path components which is beneficial especially in the NLOS situation.

Several measurements were conducted in different types of four way intersections [8] in the city of Lund and Malmö in Sweden. A single measurement is however chosen for the

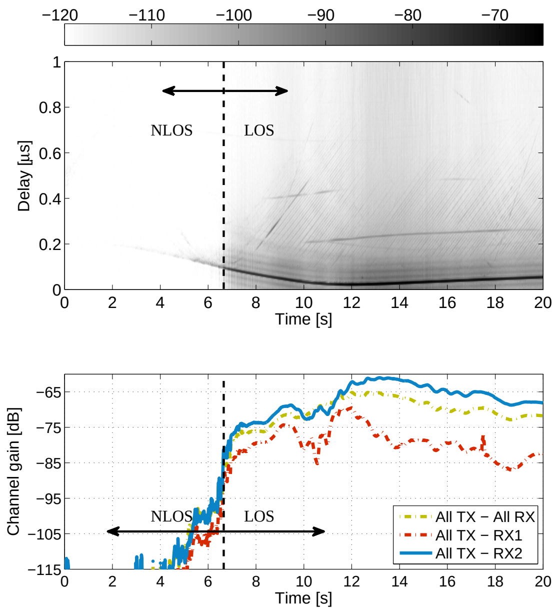

Fig. 3. Scenario-1: Averaged power delay profile (top) and channel gain of the strongest and weakest links among the 4×4 MIMO links (bottom).

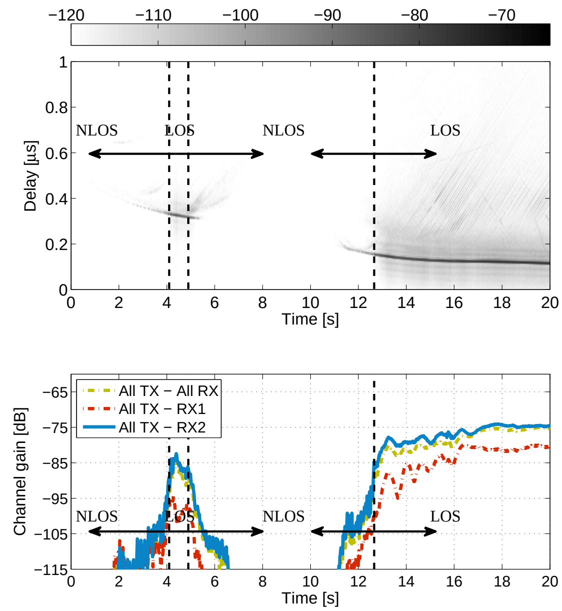

Fig. 4. Scenario-2: Averaged power delay profile (top) and channel gain of the strongest and weakest links among the 4×4 MIMO links (bottom).

analysis;

Scenario-3: when the TX and RX cars are approaching a wide-urban intersection from the streets almost perpendicular to each other. All four streets have different widths varying between $20-43$ m with different traffic conditions that makes the scenario very dynamic. Four multi-story buildings are situated at each corner of the intersection marked as B1, B2, B3 and B4, respectively (see Fig. 2).

II. Data Evaluation and Results Analysis

To analyze the radio channel properties the data evaluation is performed as follows;

A. Averaged Power Delay Profile

To analyze the impact of time-variations on the received signal power, especially in the absence of LOS, the time-varying instantaneous power-delay-profile (PDP) is derived for each time sample. The effect of small-scale fading is removed by averaging the PDPs of N_{avg} time samples. The averaged-PDP (APDP) is calculated as,

$$P_h(t_k, \tau) = \frac{1}{N_{avg}} \sum_{n=0}^{N_{avg}-1} |h(t_k + n\Delta t, \tau)|^2, \qquad (1)$$

for $t_k = \{0, N_{avg}\Delta t, ..., \lfloor N_t/N_{avg} - 1 \rfloor N_{avg}\Delta t\}$, where $h(t_k + n\Delta t, \tau)$ is the complex time varying channel impulse response derived by an inverse Fourier transform of a channel transfer function $H(f,t)$ for a single-input single-output (SISO) antenna configuration. Moreover, the $N_{avg} = 64$ is calculated as $N_{avg} = \lceil \frac{s}{v\Delta t} \rceil$, where $\Delta t = 307.2\mu$s is the time spacing between snap shots, $s =$ corresponds to the movement of the TX and RX of 10 wavelengths and v is the velocity of the TX and RX, 28 m/s, approximately.

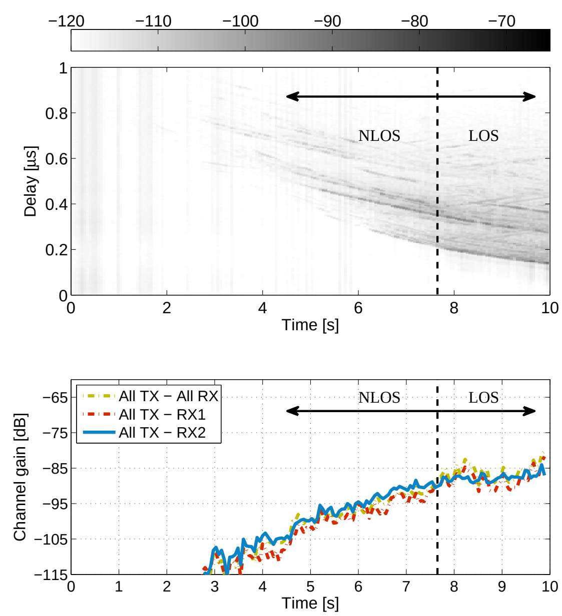

Fig. 5. Scenario-3: Averaged power delay profile (top) and channel gain of the strongest and weakest links among the 4×4 MIMO links (bottom).

We also derive the time varying channel gain, as $G(t) = \sum_\tau P_\tau(t,\tau)$, where we apply a noise threshold setting all components within 3 dB of the noise floor to zero.

The time-varying APDP and the corresponding channel gain are shown in Fig. 3 (Scenario-1), in Fig. 4 (Scenario-2) and in Fig. 5 (Scenario-3). From the APDP it is found that the channel is very poor in terms of scattering in scenario-1 and 2. It can be observed in both of the measurements that in the absence of LOS there are very few scattering objects that can provide additional propagation paths. Whereas in scenario-3 the situation is different, there exist a few significant multi-path components even in the absence of LOS originating from nearby buildings and multitude of cars waiting at traffic lights. In scenario-1 and 2 some additional power is received from the MPCs reflected from the vehicles moving next to the TX/RX, but their contribution seem to appear only when the LOS is available (see Fig. 3). It is observed that the channel gain is higher in Fig. 3 than in Fig. 4 and 5 due to the smaller distance between TX and RX.

Differences due to the antenna gain can be best appreciated in the plots of the channel gain in Fig. 3, 4 and 5 (bottom) where we show that the different TX-RX antenna pairs result in different channel gains due to different directional properties, e.g., the difference in the gain of the RX element-1 and element-2 in the forward and backward direction. The overall difference in the channel gain for the two links is higher in scenario-1 than in scenario-2 and 3 because in scenario-1 the RX is driving next to the TX, unlike in scenario-2, and the antenna gain of the RX is higher in the backward direction as compared to the forward direction. For both Scenario-1 and 2, the channel gain for all TX-RX1 is $5 - 15\,$dB lower than the all TX-RX2 link because the main gain of RX element-1 is pointing in the direction opposite to the direction of the TX. Furthermore in scenario-3 the difference in the channel gain is not so big as the four-way intersection has a rich scattering environment and there exist few MPCs wide spread in space that carry significant power in addition to the LOS component. Therefore the antenna gain do not really influence the channel gain in scenario-3. It is observed that the number of scatterers do improve the channel gain but when there exist no scattering objects then the LOS is the only major power carrying component.

B. Impact on collision avoidance applications

One of the main features of collision avoidance applications is the early warning of the possible threats to be issued few seconds in advance. Such applications require reliable communication up to a certain distance that depends on the received signal power especially in the NLOS situation. To further emphasize this and to highlight the importance of scatterers, the channel gain as a function of distance-to-collision (d_{dc}), i.e., distance from the TX to the collision point and to the RX, is shown in Fig. 6 for scenarios-1, 2 and 3. The d_{dc} can directly be related to warning time t_w, by $t_w = \frac{d_{dc}}{v_{TX}+v_{RX}}$, where v_{TX} and v_{RX} are average velocities of the TX and RX, respectively. From Fig. 6 it can be seen that the scenario 3, four-way intersection, has good signal strength at a larger d_{dc} compared to the case in scenario-1 and 2. The major difference in the channel gain in scenario-3 is due to the LOS component that is available even up to $d_{dc} = 90\,$m because of wider streets, and the buildings B2 and B3 (see Fig. 2) that provide strong reflections in the NLOS. However, scenario-2 has a few samples with high channel gain even at a distance of about 150 m due to occasional availability of LOS, mentioned in APDP plot between $4 - 5\,$s in Fig. 4 (top).

In the merging lane scenarios-1 and 2, LOS appears at a very short distance to the collision d_{dc} and no objects are

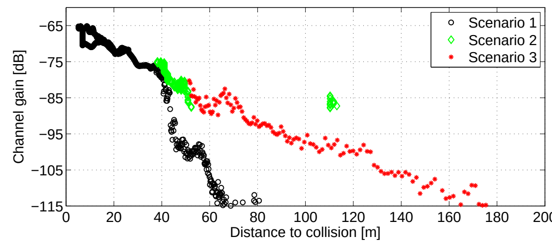

Fig. 6. Channel gain as a function of distance to collision from the TX to collision-point and to the RX averaged over all MIMO links for Scenarios 1, 2 and 3, respectively.

available in the surrounding that can contribute to improve the signal strength in the NLOS. The intersection scenario-3 on the other hand has wider geometry and buildings at the corners that act as reflection points that improve the signal strength and enable reception at larger d_{dc}. For the collision avoidance applications larger d_{dc} translates to an increased t_w, i.e., additional time to asses the hazardous situation and issue collision avoidance warnings well in time. Both the LOS as well as the scattering objects do play a critical role to enable reliable communication for such applications. Another factor that can influence the performance of the safety applications is the antenna gain as discussed in the following.

C. Directional Analysis

The propagation mechanism driving these differences in the channel gain and antenna-channel interaction can be well understood by performing a directional analysis of the measurement data. A directional analysis, similar to [15], is performed using SAGE [11]. It is assumed that the 4×4 channel matrix H can be described by a sum of L plane waves or multi-path components (MPCs) where each wave l is characterized by a complex amplitude γ_l, propagation delay τ_l, Doppler shift ν_l, DOD and DOA, respectively, for both the azimuth and the elevation angles. The parameters for 100 MPCs are estimated from the measured channel matrices and the DOA against the DOD for the estimated MPCs are presented in Fig. 7 for selected snapshots. The snapshots in scenario-1; at time instant and 17.56 s, in scenario-2; at time instant 13.51 s, and in scenario-3; at time instant 8.33 s, are chosen as example for the analysis. MPCs with a power 20 dB less than the LOS component are not shown in the figures. The propagation delay τ_l of each MPC is normalized by the propagation delay of the LOS component τ_{LOS} such that the LOS has $\tau_{LOS} = 0\,$s delay. The delay τ_l is shown as the propagation distance $S_l = c \times (\tau_l - \tau_{LOS})$ in the color bar in Fig. 7.

In the merging lane scenarios, scenario-1 and 2, there are very few interacting objects, often widely separated in space, which results in very few reflected propagation paths in addition to the LOS component. Due to the sparsity of interacting objects, the propagation distances of these MPCs are large and the signal strength is usually very low. MPCs with power $10-20\,$dB lower than the LOS component can be seen in Fig. 7, (a) and (b). These MPCs, with $1-3\,$m longer

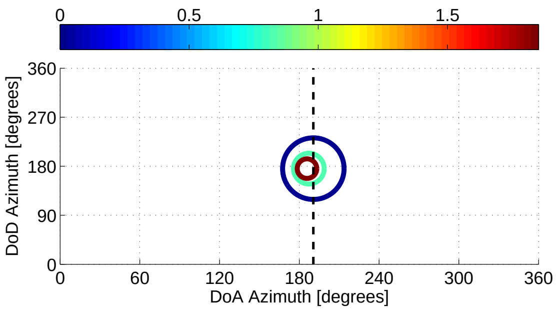

(a) scenario-1

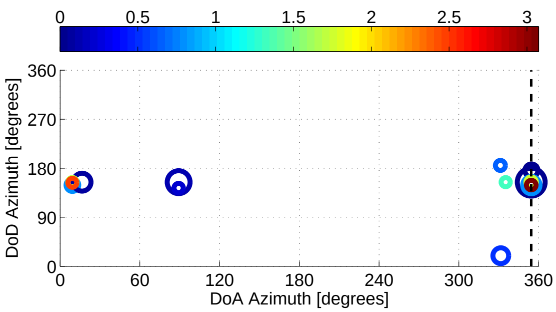

(b) scenario-2

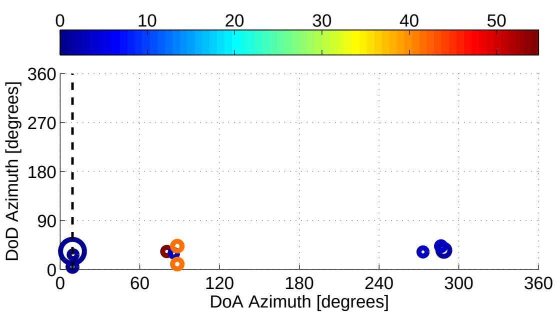

(c) scenario-3

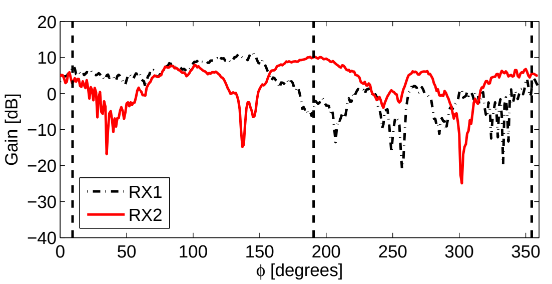

(d) Antenna gain

Fig. 7. The azimuth direction-of-arrival (DOA) and azimuth direction-of-departure (DOD) estimates for the snapshots at time instants 17.56 s (scenario-1), 13.51 s (scenario-2), and 8.33 s (scenario-3), and the azimuth antenna gain of RX element-1 and element-2 (Antenna gain) are shown. The color bar is representing the relative distance (m) w.r.t. the LOS component such that the LOS component is at 0 m. The size of the circles depicts the power carried by each MPC.

propagation distance relative to LOS propagation distance, are the paths originating from the single bounce reflection with road signs and the metallic guard rail between the ramp and the highway, and the ground reflections. Most of these MPCs are available only when there is LOS. Therefore, the received power is negligible in the absence of LOS (as shown in Fig. 3 and 4) and the LOS component constitutes most of the received power when there is a LOS between the TX and the RX (see Fig. 7).

In the four-way intersection, scenario-3, relatively higher number of MPCs are available that can be tracked even in the absence of LOS and at a larger propagation distance. These MPCs, with $1-60$ m longer propagation distance relative to LOS propagation distance, are the paths originating from the cars, a bus waiting at the traffic light, and from the buildings B1 and B2, see Fig. 2. Although there exist strong MPCs, the LOS component still dominates as it constitutes most of the power.

To analyze the variations in the received power due to the variation in the antenna gain it is important to analyze the power variations in the LOS component. The vertical dotted lines are drawn to visualize the DOA of the LOS component, the largest circle, for each snapshot to compare the differences in the antenna gain for RX element-1 and element-2 at that particular angle. As a first observation it is found that the received power can drop up to 20 dB depending upon the DOA and the differences in the antenna gain of the RX elements-1 and 2 at that angle. Comparing these results with the channel gain results in Fig. 3 (Scenario-1), in Fig. 4 (Scenario-2) and in Fig. 5 (Scenario-3), we find a direct correlation between the channel gain and the antenna radiation pattern. This implies that, even if there is a LOS between the TX and RX, the power level can drop significantly when there is a dip in the antenna pattern. This can have severe impact on the communication range and thus it needs to be considered when designing an antenna for automotive safety applications.

D. *Delay Spreads*

The root mean square (rms) delay and Doppler spreads are also important parameters in the system design. They describe how the power is spread by the channel in time and in frequency, and they are good indicators of the frequency selectivity (rms delay spread) and the time selectivity (rms Doppler spread) of the channel. Moreover, they can be related to the coherence bandwidth and coherence time as described in [16].

In this paper we consider only the time-varying rms delay spread as in [17], and we apply a threshold on the data such that we can avoid erroneous results due to spurious components. The rms Doppler spread results can be found in [7], but are not included here due to space limitation. All components below the noise floor plus 3 dB (*noise thresholding*) are set to zero.

The time-varying rms delay spread for the three scenarios (scenario-1, 2 and 3) are shown in Fig. 8. We plot the results for three different configurations, as similarly done in the previous section: in green dotted line we show the rms spreads when considering all TX antennas and all RX antennas; in red dashed line we show the results obtained when considering all TX antennas and only RX element-1; and in blue solid line we consider all TX antennas and only RX element-2.

First we observe that the rms spreads are not equal for the three links in scenario-1, clearly observable in the rms delay spread plot (Fig. 8 (a)). The link between all TX antennas and RX element-2 is the most frequency selective one, since some MPCs that are only visible to RX element-2 contribute to a large rms delay spread. The RX element-2 is focusing towards the TX (the RX driving in front of the TX), therefore, the surrounding scatterers are illuminated the most, thus resulting in strong MPCs at the RX element-2. On the other hand, when considering all RX antennas, the power of the LOS and all other MPCs is averaged over all RX antennas. Often all scatterers do not contribute to the power received at each RX antenna, therefore the averaged power of the scatterers over all RX antennas can be lower than their power in each link. Moreover, the power of the LOS component is much larger than the power of the later MPCs, so the rms delay spread is small.

We depict the time-varying rms delay spread for the second scenario (scenario-2) in Fig. 8 (b). Here we observe a similar behavior, but since now the TX is driving in front of the RX, the RX element-2 is not focusing on the TX anymore, and the number of illuminated objects is smaller than it is for the other links. Therefore, the link all TX - RX element-2 shows the smallest rms delay spread compared to the other links.

Finally in Fig. 8 (c), the rms delay spread for the third scenario is presented. A first observation is that scenario-3 is overall more frequency selective than the other two scenarios as the delay spread is large for almost all links. The main reason behind this is relatively rich scattering environment which is also observed in the APDP and DOA/DOD plots for scenario-3. For the same reason no big difference lies in the delay spread of the three links.

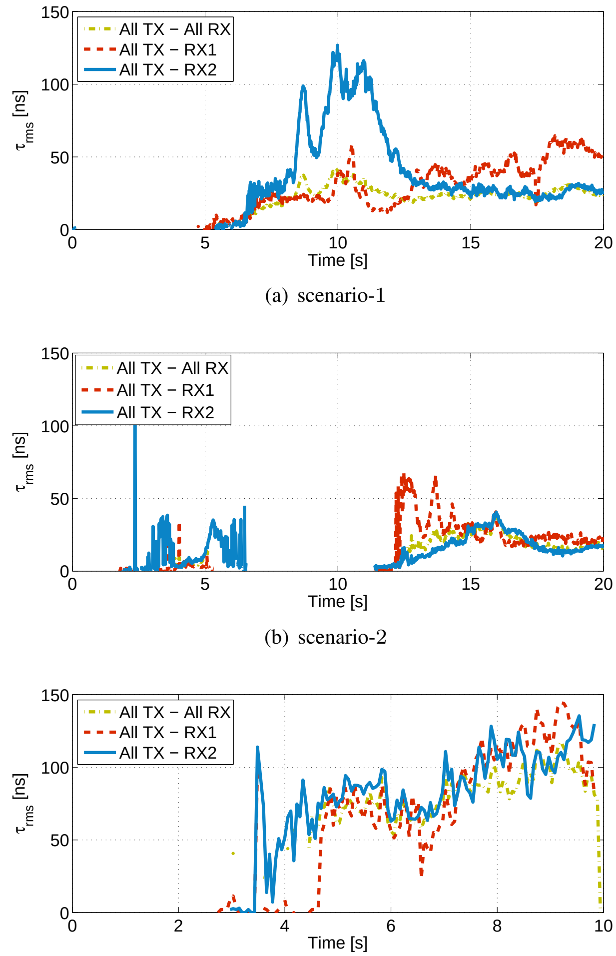

(a) scenario-1

(b) scenario-2

(c) scenario-3

Fig. 8. Time-varying rms delay spread for scenario 1, 2 and 3.

III. Summary and Conclusions

This paper presents results from a vehicle-to-vehicle measurement campaign for the safety applications targeting collision avoidance applications in merging lanes and intersection scenarios. Looking at the results for the merging lane scenario, we found that the channel gain is highly dependent on the line-of-sight (LOS) in such a sparse scattering environment. Due to lack of significant scatterers, such as road side objects and vehicles, the received power decays abruptly in the NLOS which demonstrates the importance of the LOS. On the other hand, in the four-way intersection scenario there exist some buildings at the street corners, cars and road signs that contribute to the signal strength even in the NLOS. Therefore, to summarize the discussion we can say that the street intersection scenario is similar to the merging lane scenario with slightly better propagation conditions due to availability of scatterers. This implies that the merging lane scenario is more safety critical. Moreover, the antenna radiation pattern plays an important role especially in the situation when there are few scatterers and if the antenna has a poor gain in the direction of the TX, then the received power level can drop significantly. Thus designing an antenna that has an omni-directional gain, or using multiple antennas that radiate towards different directions becomes more important for such safety critical scenarios.

References

[1] *IEEE Std. 802.11p-2010, Part 11: Wireless LAN Medium Access Control (MAC) and Physical Layer (PHY) specifications: Amendment 7: Wireless Access in Vehicular Environment*, IEEE Std., July 2010.

[2] A. F. Molisch, F. Tufvesson, J. Karedal, and C. F. Mecklenbräuker, "A survey on vehicle-to-vehicle propagation channels," in *IEEE Wireless Commun. Mag.*, vol. 16, no. 6, 2009, pp. 12–22.

[3] T. Sakaguchi, A. Uno, and S. Tsugawa, "Inter-vehicle communications for merging control," in *Vehicle Electronics Conference (IVEC '99) Proceedings of the IEEE International*, 1999, pp. 365 –370 vol.1.

[4] A. Uno, T. Sakaguchi, and S. Tsugawa, "A merging control algorithm based on inter-vehicle communication," in *Intelligent Transportation Systems. Proceedings of the IEEE/IEEJ/JSAI International Conference on*, 1999, pp. 783 –787.

[5] Q. Xu and R. Sengupta, "Simulation, analysis, and comparison of ACC and CACC in highway merging control," in *Intelligent Vehicles Symposium, 2003. Proceedings. IEEE*, june 2003, pp. 237 – 242.

[6] Y. Liu, U. Ozguner, and T. Acarman, "Performance evaluation of inter-vehicle communication in highway systems and in urban areas," in *Intelligent Transport Systems, IEE Proceedings*, vol. 153, no. 1, march 2006, pp. 63 – 75.

[7] T. Abbas, L. Bernado, A. Thiel, C. F. Mecklenbruker, and F. Tufvesson, “measurements based channel characterization for vehicle-to-vehicle communications at merging lanes on highway,” in *5th International Symposium on Wireless Vehicular Communications: WIVEC2013*. IEEE, June 2013, pp. 1–5.

[8] J. Karedal, F. Tufvesson, T. Abbas, O. Klemp, A. Paier, L. Bernadó, and A. F. Molisch, “Radio channel measurements at street intersections for vehicle-to-vehicle safety applications,” in *IEEE VTC 71st Vehicular Technology Conference (VTC 2010-spring)*, May 2010, pp. 1–5.

[9] T. Mangel, O. Klemp, and H. Hartenstein, “5.9 GHz inter-vehicle communication at intersections: a validated non-line-of-sight path-loss and fading model,” *EURASIP Journal on Wireless Communications and Networking*, vol. 2011, no. 1, p. 182, 2011.

[10] T. Abbas, J. Kredal, and F. Tufvesson, “Measurement-based analysis: The effect of complementary antennas and diversity on vehicle-to-vehicle communication,” *IEEE Antennas and Wireless Propagation Letters*, vol. 12, no. 1, pp. 309–312, 2013. [Online]. Available: http://lup.lub.lu.se/record/3516482/file/3555826.pdf

[11] B. H. Fleury, M. Tschudin, R. Heddergott, D. Dahlhaus, and K. I. Pedersen, “Channel parameter estimation in mobile radio environments using the SAGE algorithm,” *IEEE J. Select. Areas Commun.*, vol. 17, no. 3, pp. 434–450, Mar. 1999.

[12] R. Thoma, D. Hampicke, A. Richter, G. Sommerkorn, A. Schneider, U. Trautwein, and W. Wirnitzer, “Identification of time-variant directional mobile radio channels,” *Instrumentation and Measurement, IEEE Transactions on*, vol. 49, no. 2, pp. 357 –364, apr 2000.

[13] A. Thiel, O. Klemp, A. Paier, L. Bernadó, J. Karedal, and A. Kwoczek, “In-situ vehicular antenna integration and design aspects for vehicle-to-vehicle communications,” in *EUCAP*, Apr. 2010, pp. 1–5.

[14] Google earth v7.1.1.1888 (2013). [Online]. Available: http://www.google.com/earth/index.html [Accessed: 2013/08/15]

[15] T. Abbas, J. Karedal, F. Tufvesson, A. Paier, L. Bernado, and A. Molisch, “Directional analysis of vehicle-to-vehicle propagation channels,” in *2011 IEEE 73rd Vehicular Technology Conference (VTC Spring)*, May 2011, pp. 1–5.

[16] A. Molisch and M. Steinbauer, “Condensed parameters for characterizing wideband mobile radio channels,” *International Journal of Wireless Information Networks*, vol. 6, no. 3, pp. 133–154, 1999.

[17] L. Bernadó, T. Zemen, A. Paier, G. Matz, J. Karedal, N. Czink, F. Tufvesson, M. Hagenauer, A. F. Molisch, and C. F. Mecklenbräuker, “Non-WSSUS vehicular channel characterization at 5.2 GHz - Spectral divergence and time-variant coherence parameters,” in *Assembly of the International Union of Radio Science (URSI)*, August 2008, pp. 9–15.

Taimoor Abbas received his M.Sc. degree in Electronics from Quaid-i-Azam University Islamabad in 2006 and M.S. degree in Wireless Communications from Lund University in 2009. He has been with Ericsson (2008-2009) for his master thesis internship. Currently he is pursuing his PhD with radio systems group at the department of Electrical and Information Technology, Lund University. His research interests include estimation and modeling of radio channels for vehicle-to-vehicle (V2V) communications and multi-antenna systems.

Laura Bernadó received the M.Sc. degree in 2007 from the Technical University of Catalonia (UPC) in Spain, with her Master Thesis written at the Radio Communications department of the Royal Institute of Technology (KTH) in Stockholm, Sweden. In 2012 she received her doctoral degree from Vienna University of Technology. Since January 2008 she is with the Telecommunications Research Center Vienna (FTW) working as a researcher in safety-related vehicular communications projects. Her research interests are modeling of fast time-varying fading processes, and particularly characterization of non-stationarity for vehicular channels.

Andreas Thiel received the Dipl.-Ing. (M.Sc.) degree in electrical engineering with special subjects high frequency and antenna technology from the University of Hannover in 2002. Since then he has been working in the Forward Engineering department for antennas and connectivity and recently became Technical Manager for Antenna and C2C-Communication at Delphi Deutschland GmbH in Bad Salzdetfurth, Germany.

Christoph Mecklenbräuker received the Dipl-Ing. degree in Electrical Engineering from Vienna University of Technology in 1992 and the Dr.-Ing. degree from Ruhr-University of Bochum in 1998, respectively. From 1997-2000, he worked for Siemens AG Austria and was a delegate to the Third Generation Partnership Project (3GPP). From 2000 to 2006, he was a senior researcher at the Telecommunications Research Center Vienna (FTW). In 2006, he joined Vienna University of Technology as a full professor. Since July 2009, he leads the Christian Doppler Laboratory for Wireless Technologies for Sustainable Mobility. C. Mecklenbruker is a member of the IEEE, the Antennas and Propagation Society, the Vehicular Technology society, the Signal Processing society, and EURASIP.

Fredrik Tufvesson received his Ph.D. in 2000 from Lund University in Sweden. After almost two years at a startup company, Fiberless Society, he is now associate professor at the department of Electrical and Information Technology, Lund University. His main research interests are channel measurements and modeling for wireless communication, including channels for both MIMO and UWB systems. Beside this, he also works on distributed antenna systems and radio based positioning.